Electronic Supplementary Information for

A Novel Strategy of Constructing Artificial Light-Harvesting System based on Supramolecular Organic Framework for Photocatalysis

Ying Wang, Chao-Qun Ma, Xin-Long Li, Rui-Zhi Dong, Hui Liu, Rong-Zhou Wang, Shengsheng Yu and Ling-Bao Xing*

School of Chemistry and Chemical Engineering, Shandong University of Technology, Zibo 255000, P. R. China

*Corresponding author: lbxing@sdut.edu.cn.

Experimental

Materials: Unless specifically mentioned, all chemicals are commercially available and were used as received.

Characterizations: ^{1}H NMR spectra were recorded on a Bruker Advance 400 spectrometer (400 MHz) at 298 K, and the chemical shifts (δ) were expressed in ppm, and J values were given in Hz. UV-vis spectra were obtained on a Shimadzu UV-1601PC spectrophotometer in a quartz cell (light path 10 mm) at 298 K. Steady-state fluorescence measurements were carried out using a Hitachi 4500 spectrophotometer. Dynamic light scattering (DLS) and zeta potential are measured on Malvern Zetasizer Nano ZS90. Transmission electron microscopy (TEM) images were obtained on a JEM 2100 operating at 120 kV. Samples for TEM measurement were prepared by dropping the mixed aqueous solution on a carbon-coated copper grid (300 mesh) and drying by slow evaporation. Hamamatsu absolute quantum yield measuring instrument Quantaurus-QY was used to obtain fluorescence quantum yields. The photocatalytic reaction was performed on WATTCAS Parallel Photocatalytic Reactor (WP-TEC-HSL) with 10W COB LED.

Energy-transfer efficiency calculation: The energy-transfer efficiency (Φ_{ET}) was calculated from excitation fluorescence spectra through the equation S1: $\Phi_{ET} = 1 - I_{DA} / I_{D}$. Where I_{DA} and I_{D} are the fluorescence intensities of the emission of SOF+DBT assembly (donor and acceptor) and SOF (donor) respectively when excited at 365 nm. The energy-transfer efficiency (Φ_{ET}) was calculated as 70.2% in an aqueous environment, measured under the condition of [MV-TPE] = 2.0×10^{-5} M, [NA-TPE] = 2.0×10^{-5} M, [CB[8]] = 8.0×10^{-5} M, [DBT] = 2.0×10^{-7} M.

The second step energy-transfer efficiency (Φ_{ET}) was calculated from excitation fluorescence spectra through the equation: $\Phi_{ET} = 1 - I_{DA} / I_{D}$. Where I_{DA} and I_{D} are the fluorescence intensities of the emission of SOF+DBT+SR101 assembly (donor and acceptor) and SOF+DBT assembly (donor) respectively when excited at 365 nm. The Φ_{ET} of the second step energy transfer process was calculated as 44.5% in an aqueous environment, measured under the condition of [MV-TPE] = 2.0×10^{-5} M, [NA-TPE] = 2.0×10^{-5} M, [CB[8]] = 8.0×10^{-5} M, [DBT] = 2.0×10^{-7} M, [SR101]=2.0×10^{-6} M.

Antenna effect calculation: The antenna effect was calculated based on the excitation spectra using equation S2: Antenna effect = $(I_{DA,365} - I_{D,365}) / I_{DA,585}$. Where $I_{D,365}$ and $I_{DA,585}$ are the fluorescence intensities at 560 nm with the excitation of the donor at 365 nm and the direct excitation of the acceptor, respectively. $I_{DA,365}$ is the fluorescence intensities of the SOF, which was normalized with the SOF+DBT assembly at 486 nm. The antenna effect value was calculated as 12.3 in water, measured under the condition of [MV-TPE] = 2.0×10^{-5} M, [NA-TPE] = 2.0×10^{-5} M, [CB[8]] = 8.0×10^{-5} M, [DBT] = 2.0×10^{-7} M.

The second step antenna effect was calculated based on the excitation spectra using the equation: Antenna effect = $(I_{DA,365} - I_{D,365}) / I_{DA,585}$. Where $I_{D,365}$ and $I_{DA,585}$ are the fluorescence intensities with the excitation of the donor at 365 nm and the direct excitation of the acceptor at 560 nm, respectively. $I_{DA,365}$ is the fluorescence intensities at 614 nm of the SOF+DBT assembly, which was normalized with the SOF+DBT+SR101 assembly at 561 nm. The antenna effect value was calculated as 1.8 in water, measured under the condition of [MV-TPE] = 2.0×10^{-5} M, [NA-TPE] = 2.0

$\times 10^{-5}$ M, [CB[8]] = 8.0×10^{-5} M, [DBT] = 2.0×10^{-7} M, [SR101]=2.0×10^{-6} M.

General procedure for the aerobic cross-dehydrogenative coupling (CDC) reaction: N-phenyl-1, 2, 3, 4-tetrahydroisoquinoline or its derivatives (0.05 mmol, 1 equiv.) and indole and its derivative (0.1 mmol, 2 equiv.) were dissolved in the freshly prepared SOF+DBT+SR101 assembly solution (0.45 mol%, 3 mL, [MV-TPE] = 7.5×10^{-5} M, [NA-TPE] = 7.5×10^{-5} M, [CB[8]] = 3.0×10^{-4} M, [DBT] = 7.5×10^{-7} M, [SR101]=7.5×10^{-6} M). The mixture was irradiated by a UV lamp (10 W, 365 nm) at room temperature under ambient air conditions. Then the mixture was extracted with ethyl acetate, and the combined organic layer was dried with anhydrous Na_2SO_4. Then the organic solvent was concentrated in vacuo and purified by flash column chromatography with petroleum ether/ethyl acetate to afford the products. The yield of the reaction was calculated by the equation: yield (%) = number of moles of the product obtained/number of moles of the feeded reactant × 100%. The ‘number of moles of the product’ is calculated from the characteristic proton signal integration of the target product divided by the corresponding proton number, and the ‘number of moles of the feeded reactant’ is the sum number of the remaining substrate, target product and by-products calculated by the same way.

Synthesis of N-phenyl-1, 2, 3, 4-tetrahydroisoquinoline: CuI (200 mg, 1.0 mmol), potassium phosphate (4.25 g, 20 mmol), 2-propanol (10 mL), ethylene glycol (1.11 mL), 1,2,3,4-tetrahydroisoquinoline (2.0 mL, 15 mmol), iodobenzene (1.12 mL, 10 mmol) were added to the reaction flask in turn, evacuated and replaced with nitrogen three times, and then reacted at 90 °C for 24 h. After the reaction, the mixture was cooled to room temperature and 25 mL of water was added. Then the mixture was extracted with ethyl acetate. The organic phases were combined, washed with brine, and dried over anhydrous sodium sulfate. The solvent was distilled off under reduced pressure, and the pure yellow product was obtained by silica gel column chromatography.

Synthesis of NA-TPE: Synthesis of 4Br-TPE was according to the literature procedure as shown in Scheme S1[S1]. 4Br-TPE (0.12 g, 0.18 mmol), 6-methoxy-2-naphthaleneboronic acid (0.18 g, 0.90 mmol) and ($Pd(Ph_3)_4$) (0.04 g, 0.036 mmol) were added to the mixed solution of THF and toluene (7:1). After the addition of 2 mL (2 mol/L) potassium carbonate solution, the mixture was refluxed under N_2 atmosphere for 2 days. The reaction mixture was then cooled to room temperature and the solvent was removed under reduced pressure. The precipitate was dissolved in CH_2Cl_2 and the solution was washed with water for three times. After the solvent is removed, the product can be obtained by silica gel chromatography (petroleum ether:ethyl acetate = 20:1, v/v) as a green solid. ^1H NMR (400 MHz, $CDCl_3$) δ 7.97 (d, J = 9.3 Hz, 4H), 7.77 (d, J = 8.0 Hz, 8H), 7.73 – 7.67 (m, 4H), 7.52 (t, J = 6.0 Hz, 8H), 7.24 – 7.10 (m, 16H), 3.93 (s, 12H).

Synthesis of MV-TPE: Synthesis of 4V-TPE was according to the literature procedure as shown in Scheme S2[S2]. 4V-TPE (0.1 g, 0.09 mmol) was dissolved in CH_3CN (20 mL) and CH_3I (0.28 mL) was added. The mixture was stirred at 45 °C for 12 h. After the mixture was cooled down to room temperature, ammonium hexafluorophosphate was added and the precipitate was filtered and washed with CH_3CN. Then the precipitate was dissolved in H_2O and tetrabutylammonium chloride (TBACl) was added. The precipitate was filtered and washed with water. Then the solid was dried under a vacuum overnight to yield an orange-yellow solid product. ^1H NMR (400 MHz, D_2O) δ 9.37 (d, J = 6.4 Hz, 8H), 9.08 (d, J = 6.3 Hz, 8H), 8.72 (d, J = 6.4 Hz, 8H), 8.61 (d, J = 6.4 Hz, 8H), 7.76 (d, J = 8.2 Hz, 8H), 7.68 (d, J = 8.3 Hz, 8H), 4.52 (s, 12H). HRMS (ESI): m/z $[M-8Cl]^{8+}$ calculated for $C_{70}H_{60}N_8$: 126.6633; found: 126.6646.

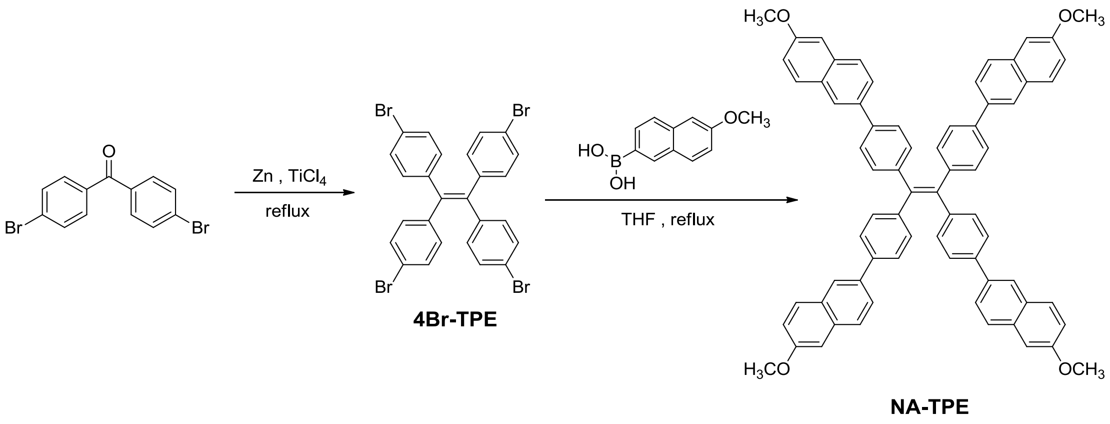

Scheme S1. Synthetic route of NA-TPE.

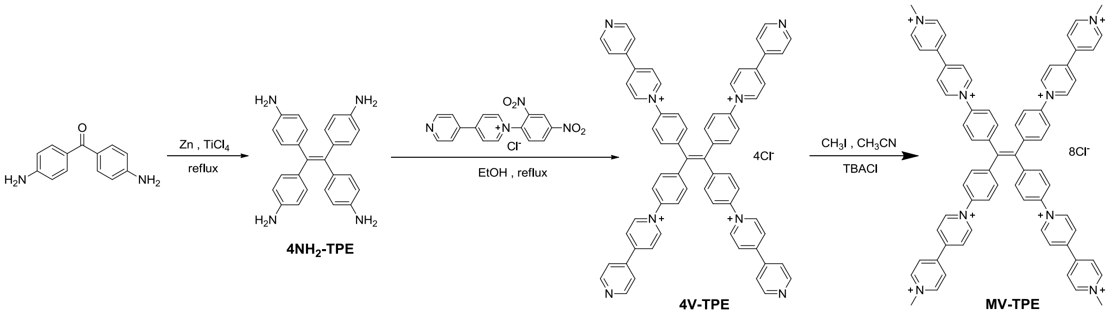

Scheme S2. Synthetic route of MV-TPE.

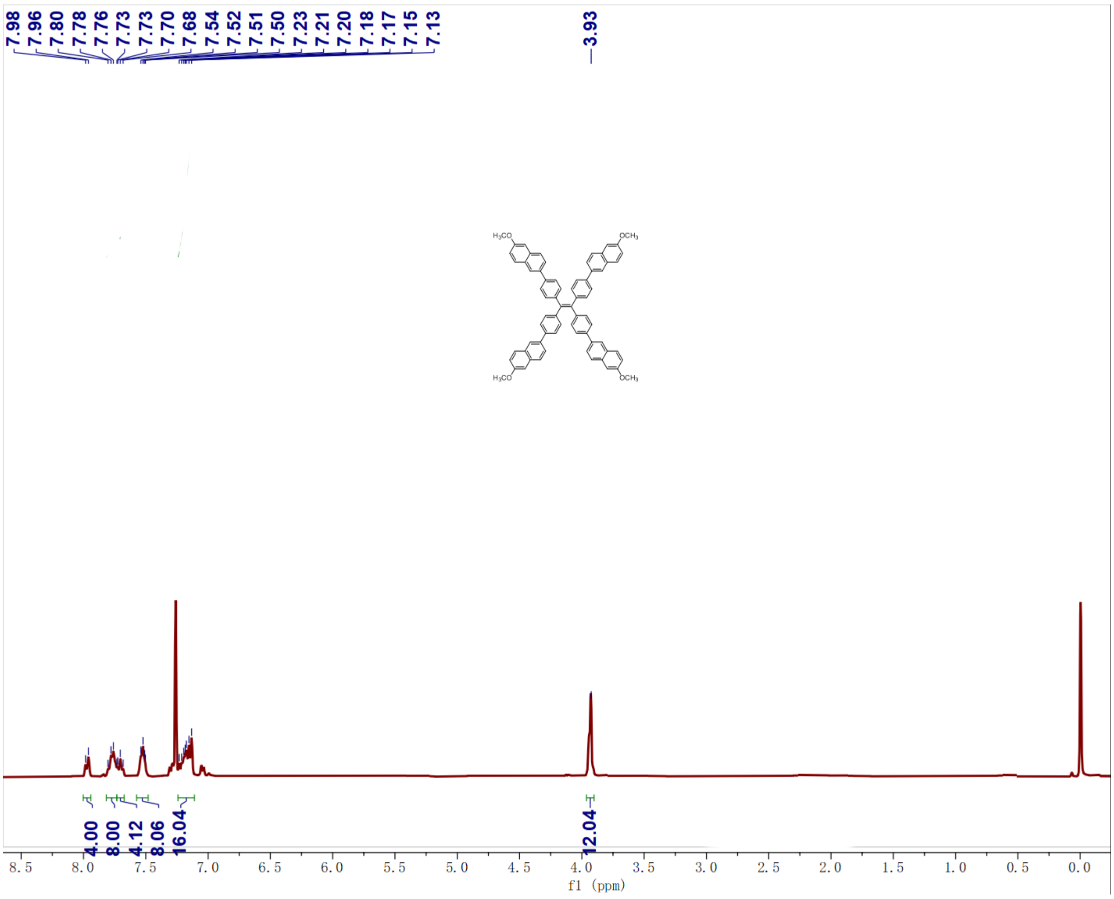

Fig. S1 ^{1}H NMR spectrum of **NA-TPE** in $CDCl_3$.

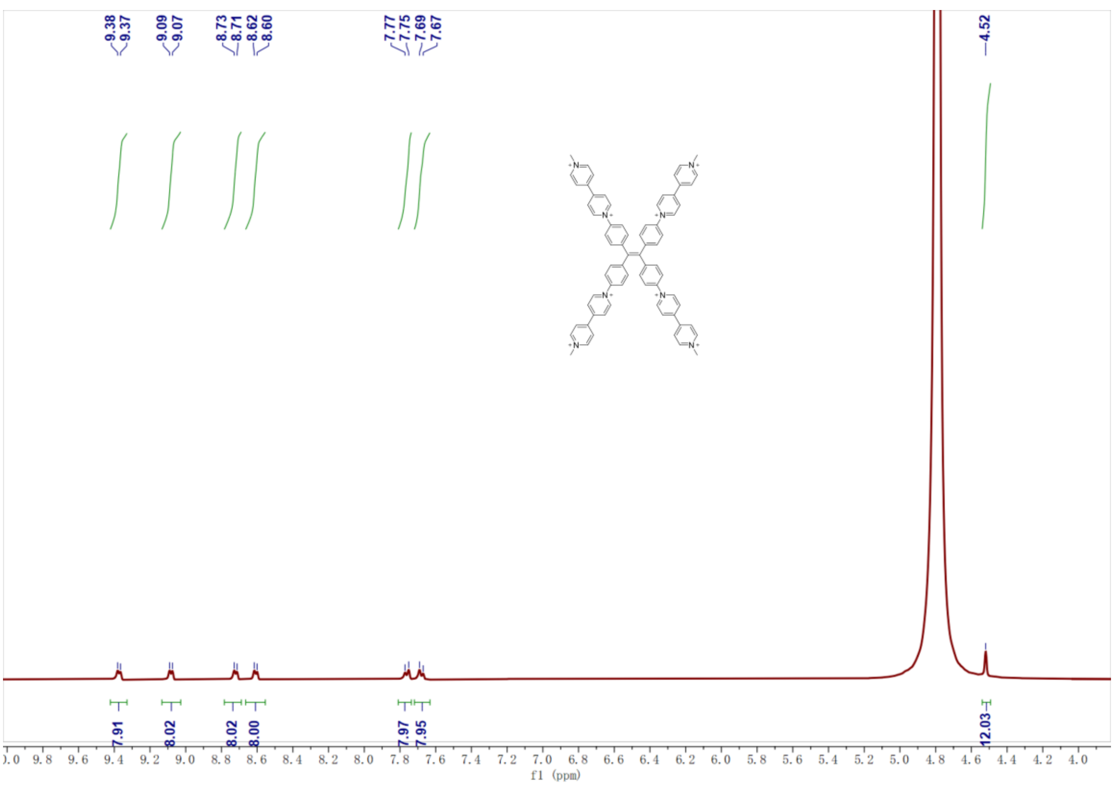

Fig. S2 ^{1}H NMR spectrum of **MV-TPE** in D_2O.

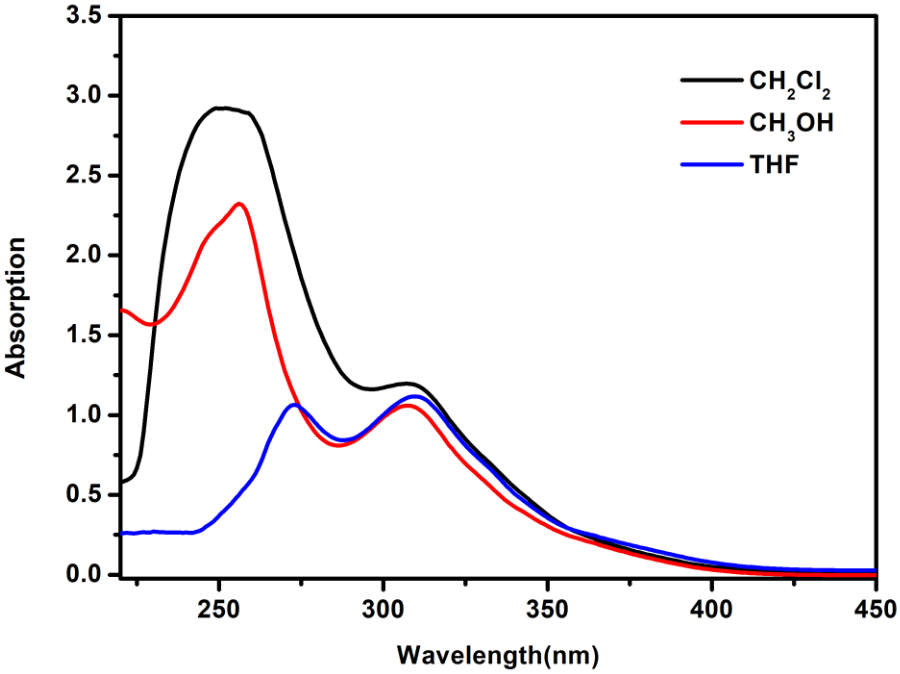

Fig. S3 UV-vis absorption spectra of NA-TPE in CH_2Cl_2, CH_3OH, and THF.

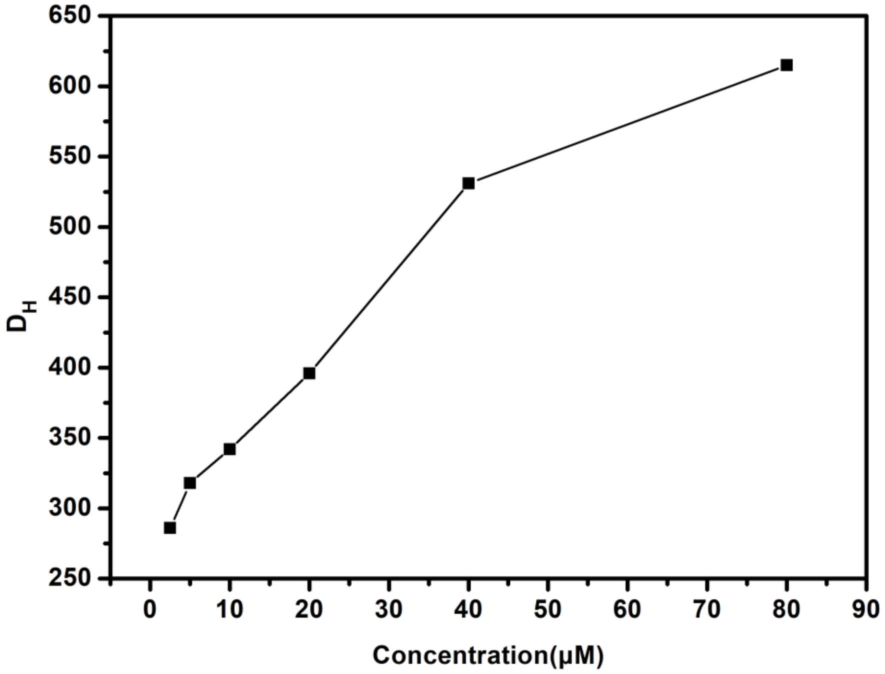

Fig. S4 DLS data of SOF (MV-TPE+NA-TPE+CB[8]=1:1:4) at different concentrations.

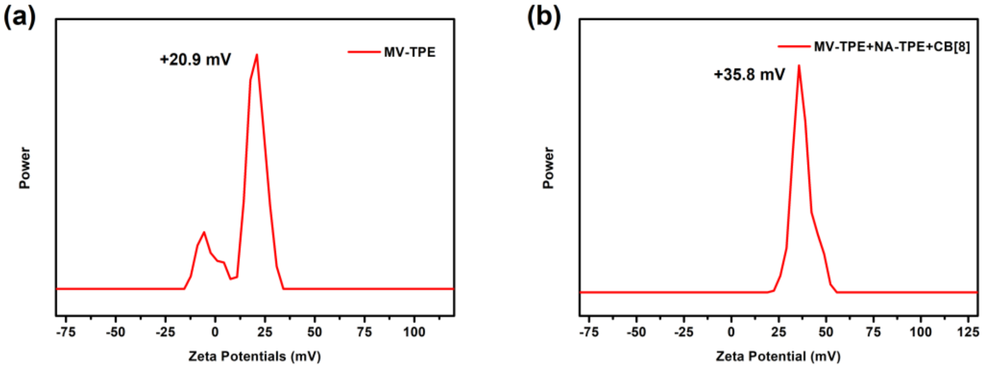

Fig. S5 Zeta potential of (a) MV-TPE and (b) MV-TPE+NA-TPE+CB[8] (1:1:4).

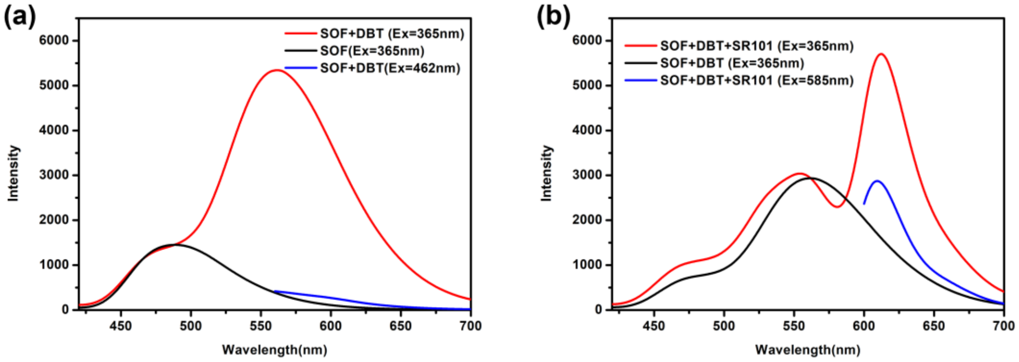

Fig. S6 (a) The UV-vis absorption spectra of DBT and fluorescence emission spectra of SOF. (b) The UV-vis absorption spectra of SR101 and fluorescence emission spectra of SOF+DBT (λ_{ex} = 365 nm).

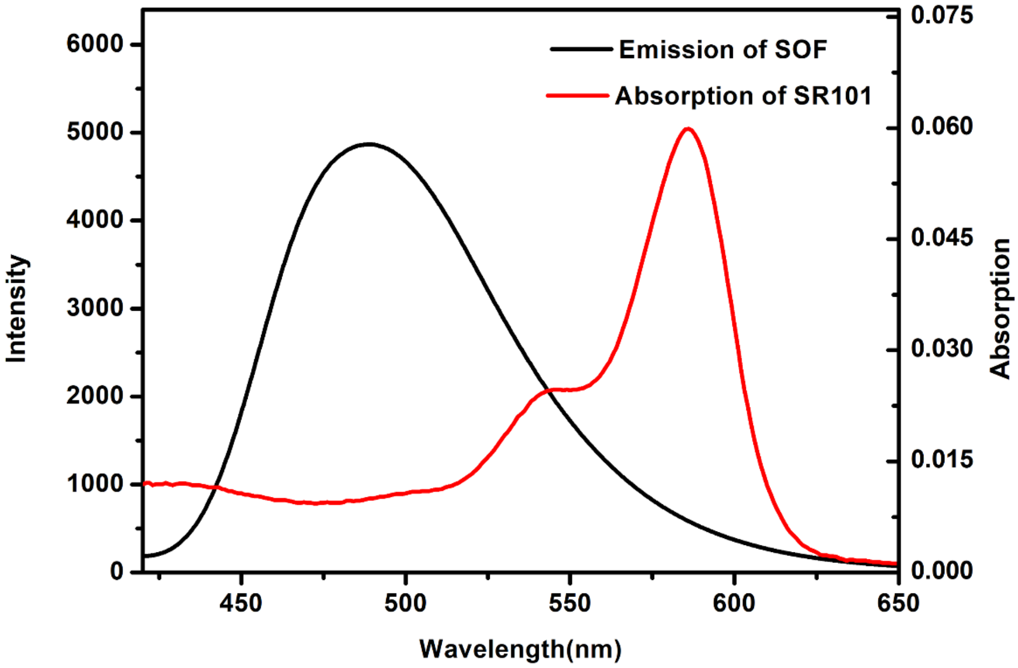

Fig. S7 The UV-vis absorption spectra of SR101 and fluorescence emission spectra of SOF (λ_{ex} = 365 nm).

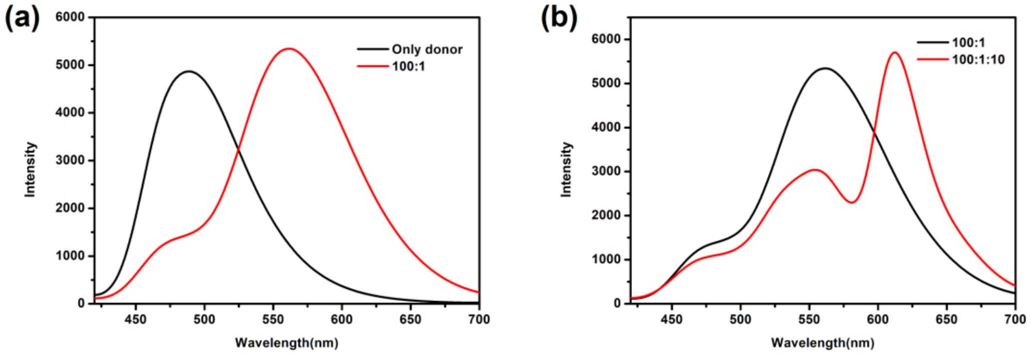

Fig. S8 Fluorescence emission spectra of (a) SOF and SOF+DBT (100:1) in water. (b) (a) SOF+DBT (100:1) and SOF+DBT+SR101 (100:1:10) in water.

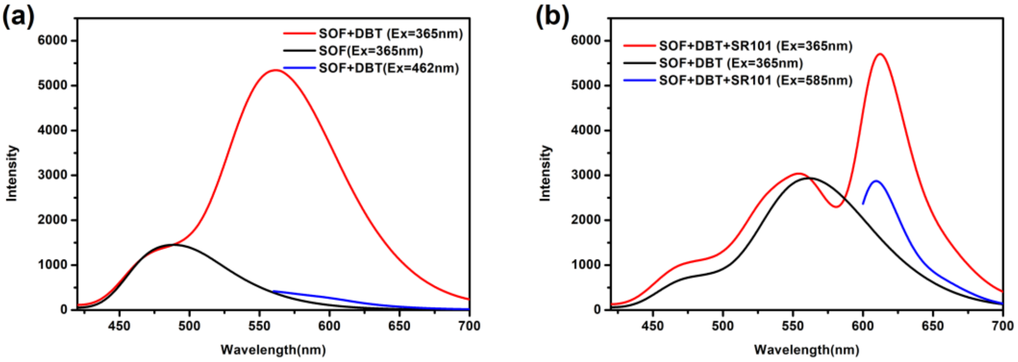

Fig. S9 (a) Fluorescence emission spectra of SOF in aqueous solution, black line, which was normalized according to the fluorescence intensity at 486 nm of the red line (λ_{ex} = 365 nm). The red line represents the fluorescence emission spectra of SOF+DBT. The blue line represents the fluorescence emission spectra of SOF+DBT when excited at 462 nm. (b) Fluorescence emission spectra of SOF+DBT in aqueous solution, black line, which was normalized according to the fluorescence intensity at 560 nm of the red line (λ_{ex} = 365 nm). The red line represents the fluorescence emission spectra of SOF+DBT+SR101. The blue line represents the fluorescence emission spectra of SOF+DBT when excited at 585 nm. ([MV-TPE] = 2.0×10^{-5} M, [NA-TPE] = 2.0×10^{-5} M, [CB[8]] = 8.0×10^{-5} M, [DBT] = 2.0×10^{-7} M, [SR101]=2.0×10^{-3} M).

Table S1. Comparative data on catalyst dosage for the CDC reaction of N-phenyl-1,2,3,4-tetrahydroisoquinoline with indole.

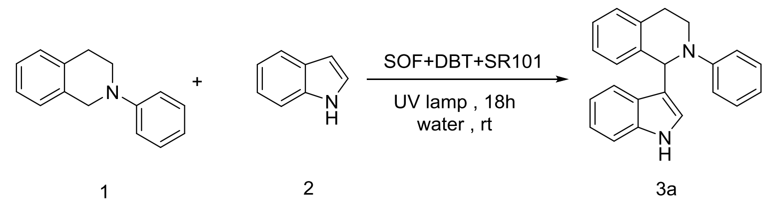

Entry	Conditions	Light irradiation	Yield/%
1	0.15mol%	Yes	61%
2	0.30mol%	Yes	78%
3	0.45mol%	Yes	87%

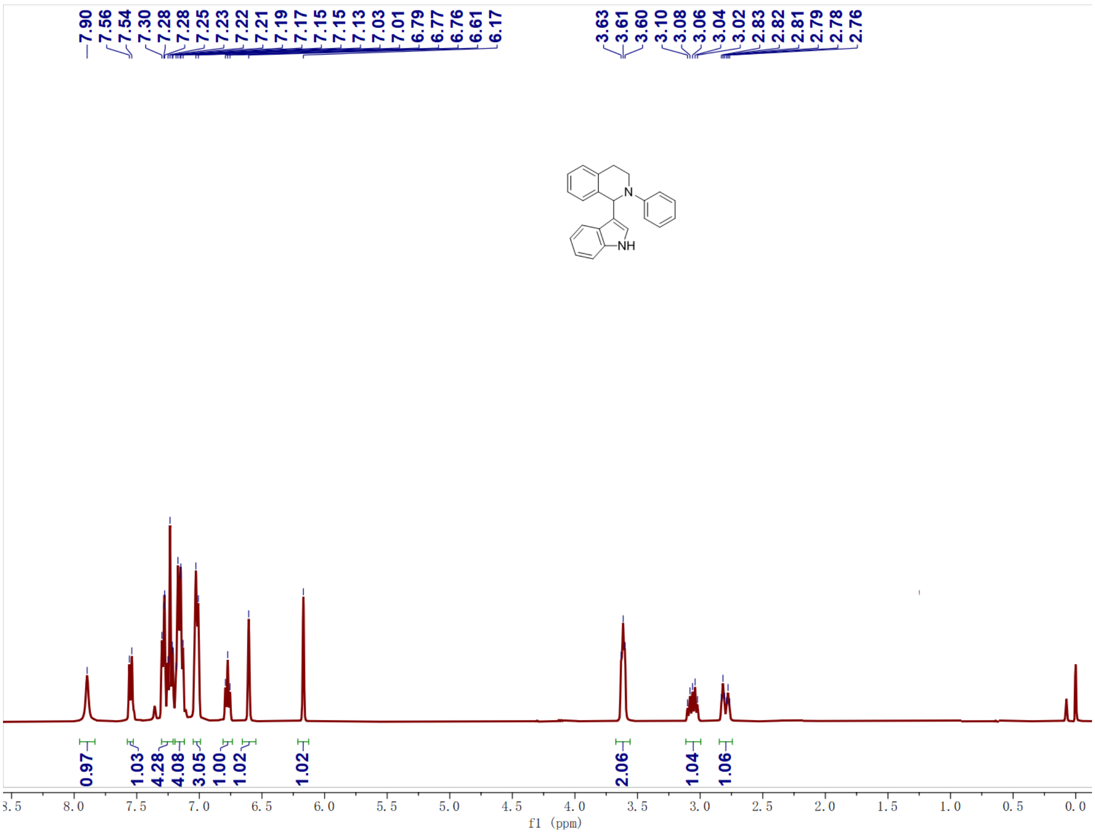

Fig. S10 ^{1}H NMR spectrum of **3a** in $CDCl_3$.

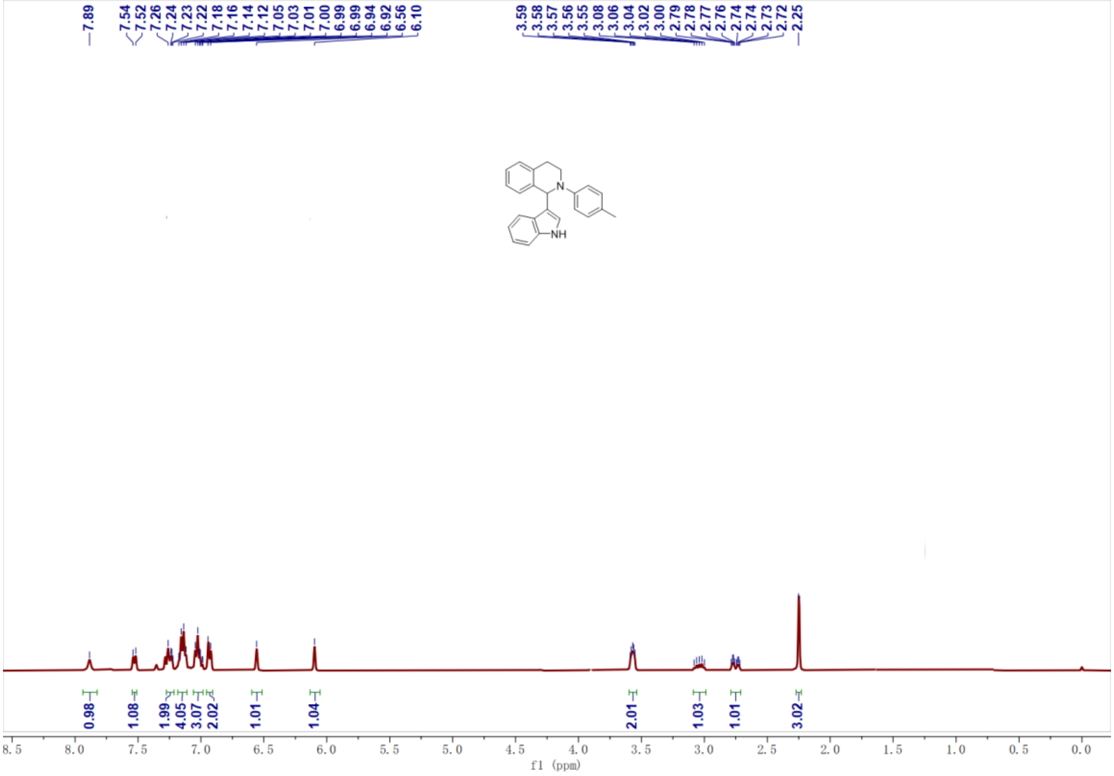

Fig. S11 ^{1}H NMR spectrum of **3b** in CDCl$_3$.

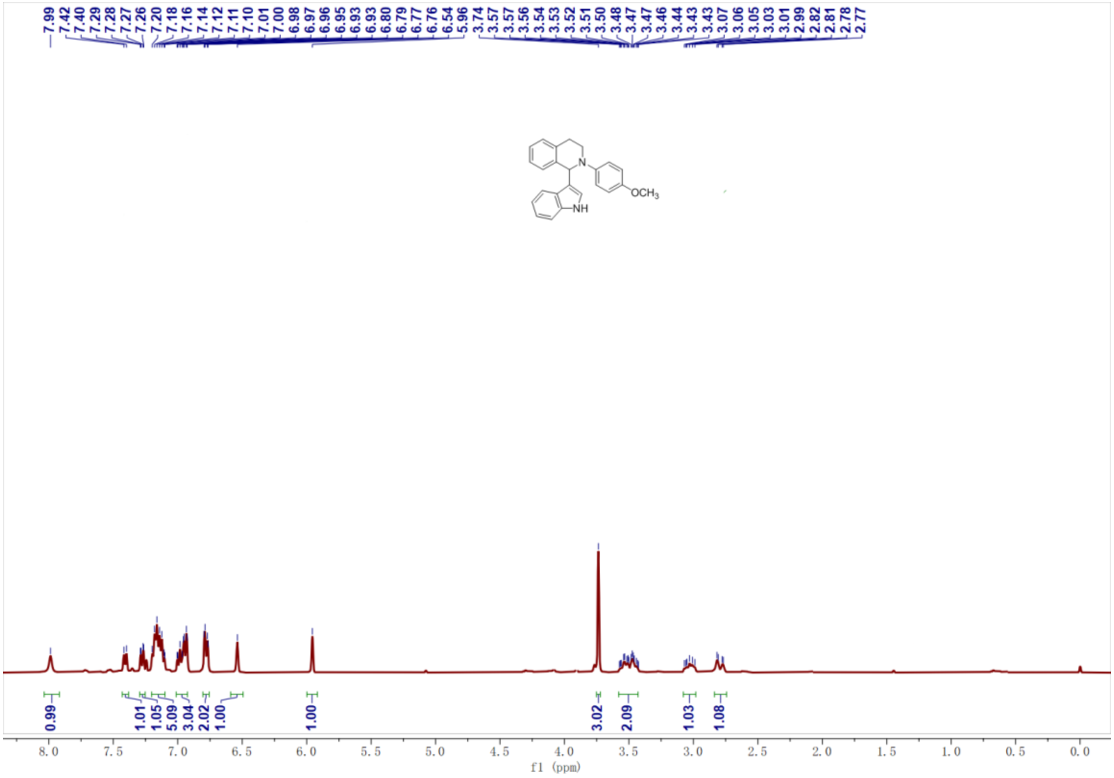

Fig. S12 ^{1}H NMR spectrum of **3c** in CDCl$_3$.

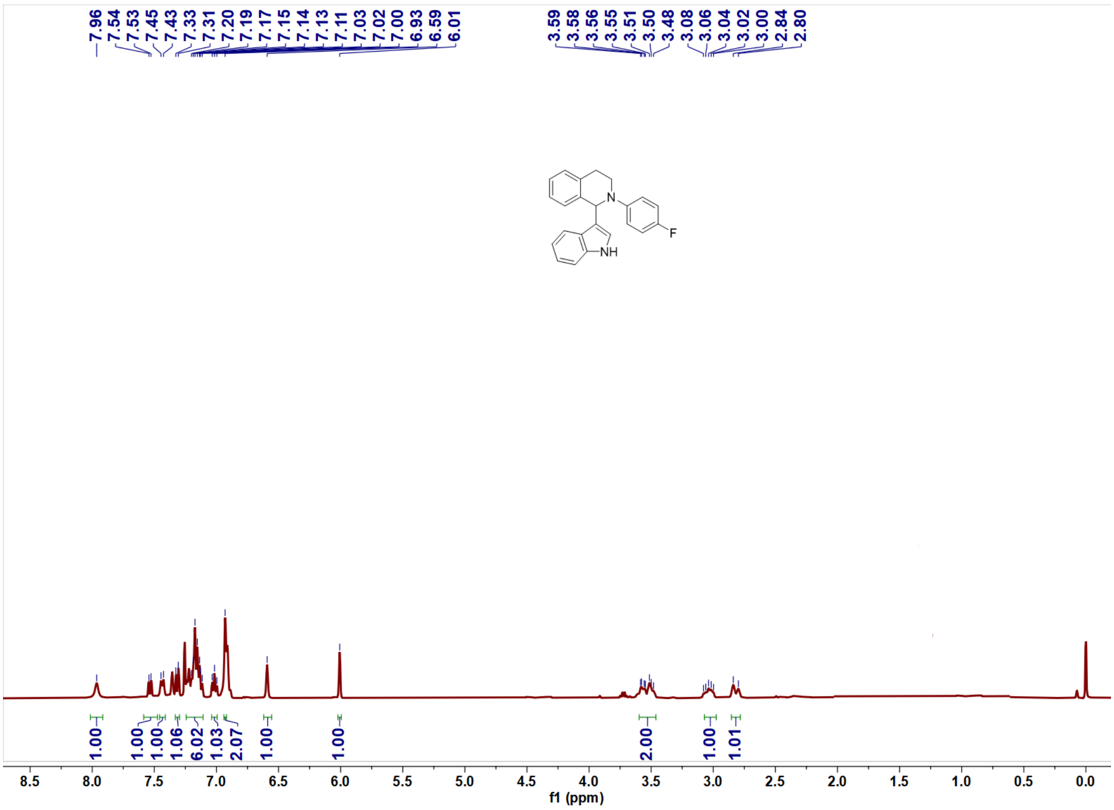

Fig. S13 ^{1}H NMR spectrum of **3d** in $CDCl_3$.

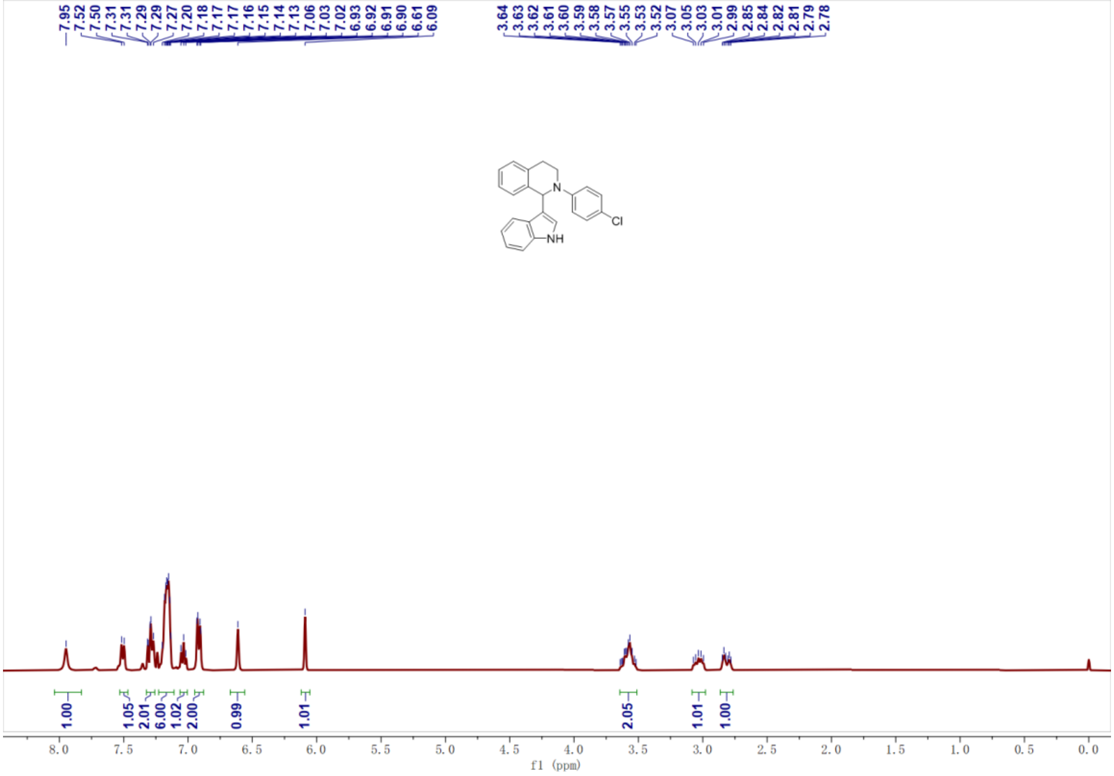

Fig. S14 ^{1}H NMR spectrum of **3e** in $CDCl_3$.

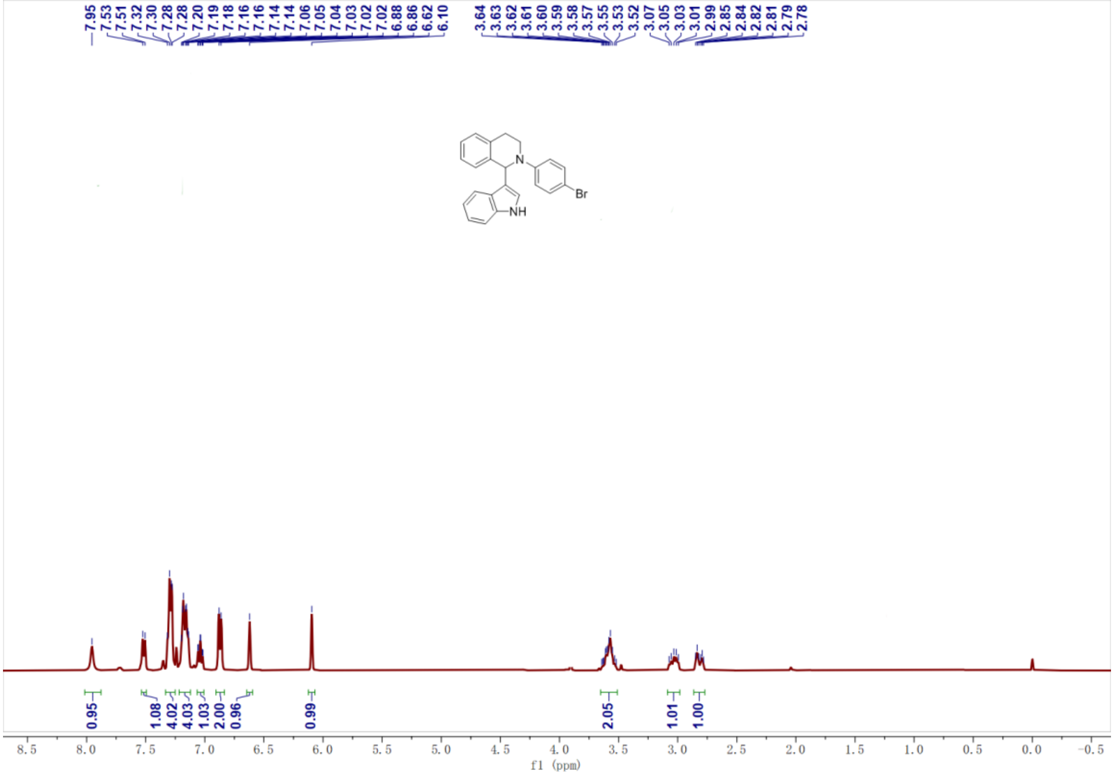

Fig. S15 ^{1}H NMR spectrum of **3f** in $CDCl_3$.

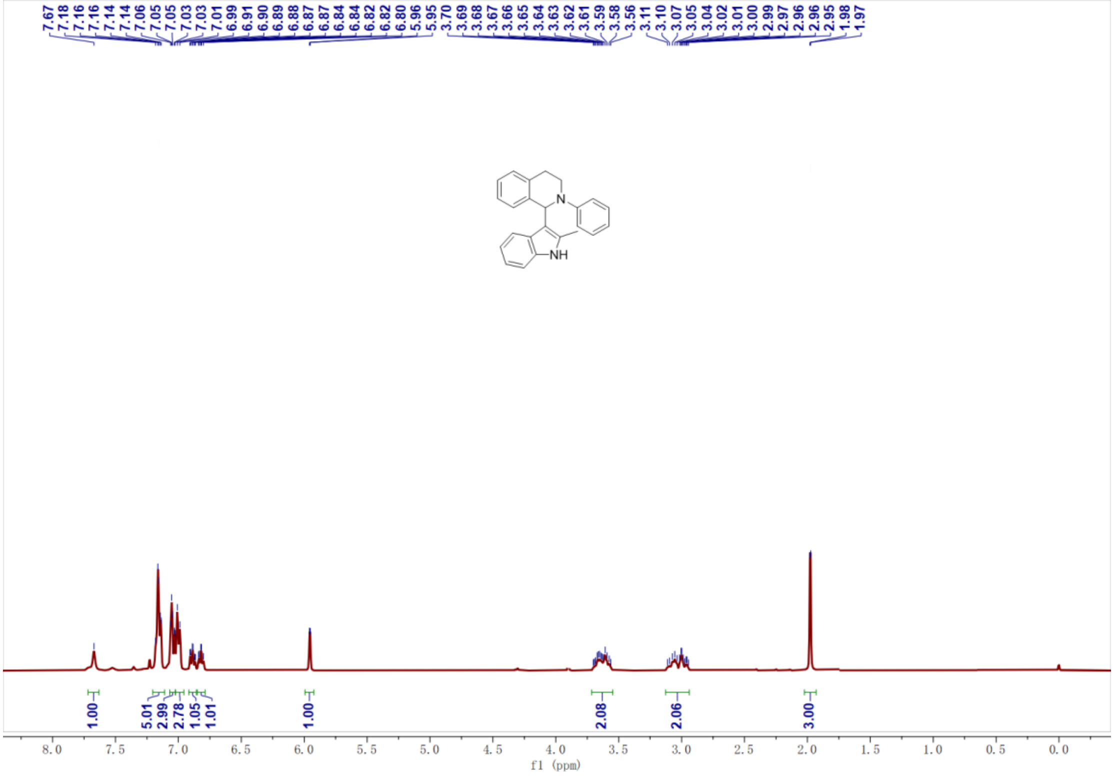

Fig. S16 ^{1}H NMR spectrum of **3g** in CDCl$_3$.

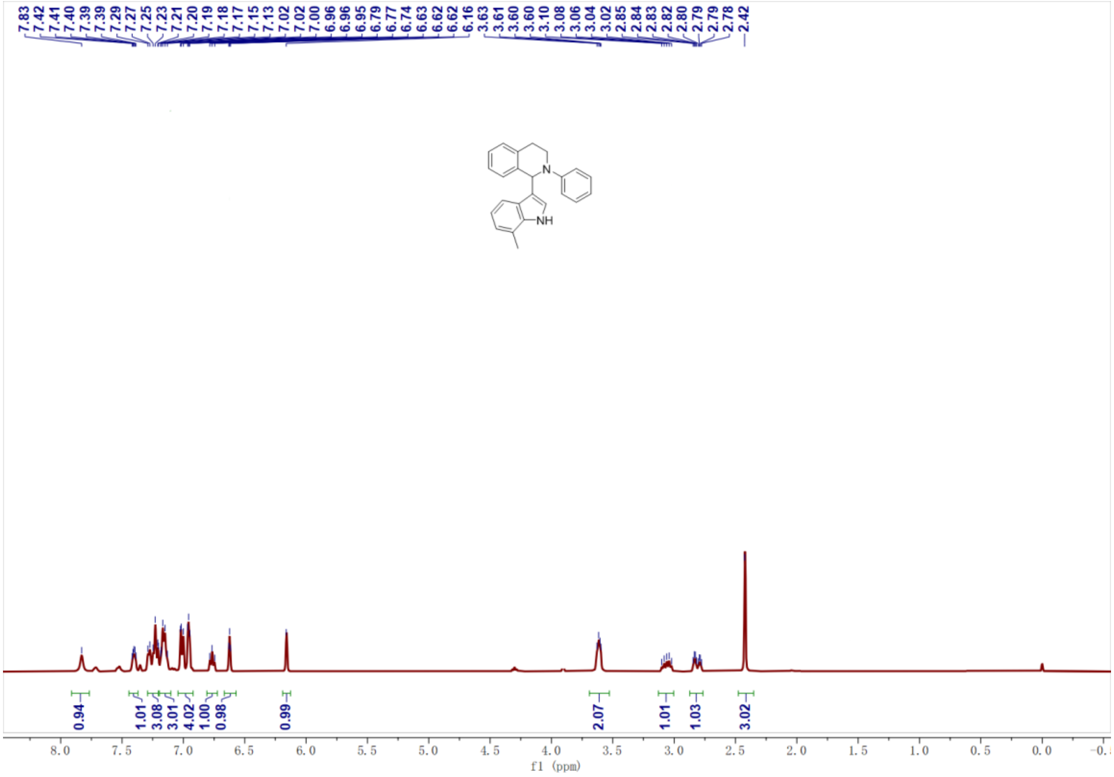

Fig. S17 ^{1}H NMR spectrum of **3h** in $CDCl_3$.

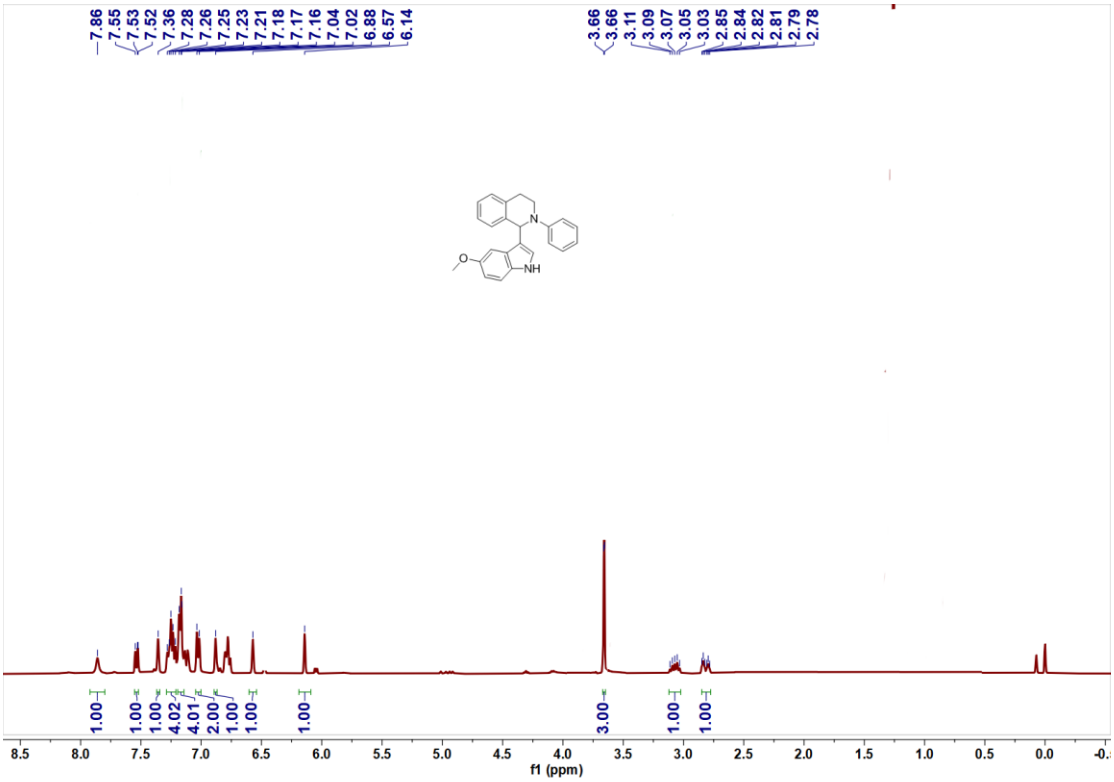

Fig. S18 ^1H NMR spectrum of **3i** in $CDCl_3$.

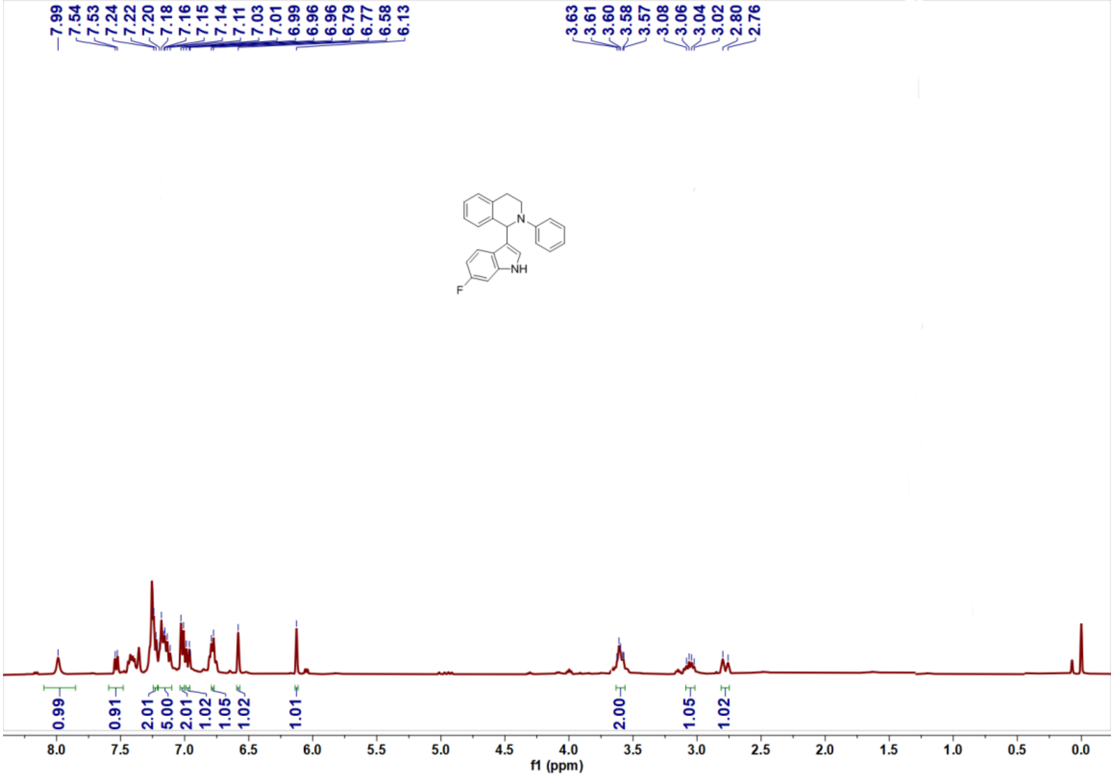

Fig. S19 ^{1}H NMR spectrum of **3j** in CDCl$_3$.

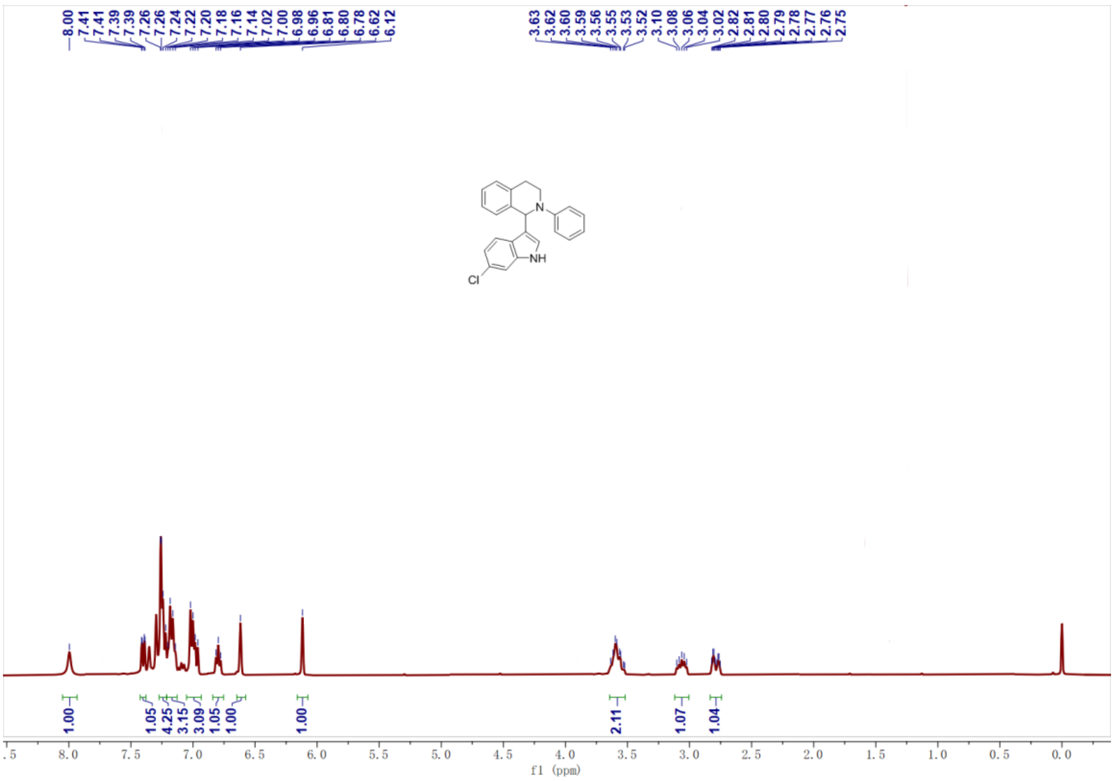

Fig. S20 ^{1}H NMR spectrum of **3k** in $CDCl_3$.

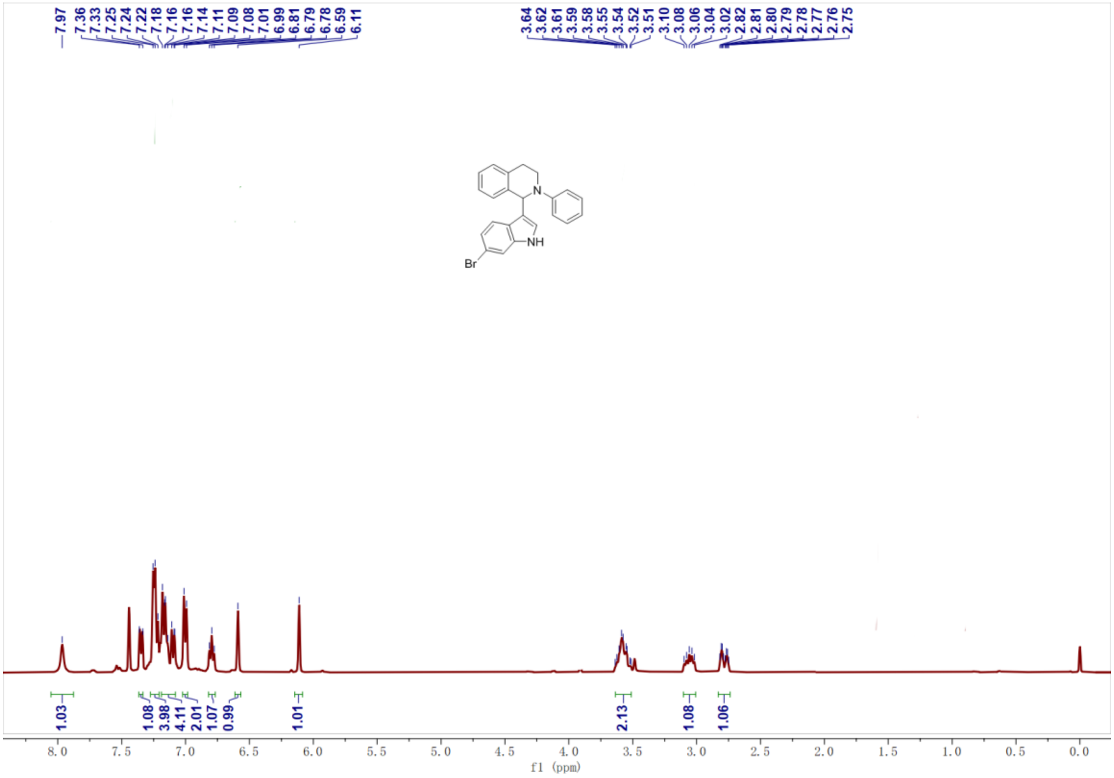

Fig. S21 ^{1}H NMR spectrum of **3l** in $CDCl_3$.

[S1] T. Zhang, Y. Li, Z. Zheng, R. Ye, Y. Zhang, R. T. K. Kwok, J. W. Y. Lam and B. Z. Tang, *J. Am. Chem. Soc.,* 2019, **141**, 5612-5616.

[S2] S. Q. Xu, X. Zhang, C. B. Nie, Z. F. Pang, X. N. Xu and X. Zhao, *Chem. Commun.*, 2015, **51**, 16417-16420.